Ionics
https://doi.org/10.1007/s11581-018-2462-1

ORIGINAL PAPER

A highly sensitive electrochemical sensor for bisphenol A using cetyltrimethylammonium bromide functionalized carbon nanohorn modified electrode

Jing Zhang [1,2] · Xiaojian Xu [1] · Zhidong Chen [1]

Received: 7 August 2017 / Revised: 17 January 2018 / Accepted: 19 January 2018

Abstract
A highly sensitive electrochemical bisphenol A (BPA) sensor was developed based on cetyltrimethylammonium bromide (CTAB) functionalized carbon nanohorn (CNH) modified electrode. CNH was carboxylated and could well disperse in water, and CNH-modified electrode showed enhanced electron transfer and high conductivity. Carboxylic CNH was functionalized with a cationic surfactant (CTAB) via the electrostatic interaction. CTAB functionalized CNH (CTAB-CNH) suspension was dropped onto glassy carbon electrode (GCE) to fabricate CTAB-CNH/GCE. Combined with preconcentration of BPA in the long alkane chain of CTAB via hydrophobic interaction and electrocatalytic activity of CNH, CTAB-CNH/GCE had high electrochemical response toward the oxidation of BPA, and an electrochemical BPA sensor was constructed on CTAB-CNH/GCE using differential pulse voltammetry. Under optimal experimental conditions, the designed sensor exhibited a wide linear response to BPA ranging from 0.01 to 30 μmol/L with a low detection limit of 5.6 nmol/L at a signal-to-noise ratio of 3. The proposed sensor has good reproducibility, reusability, and anti-interference properties, and was successfully applied to detect BPA in real samples with satisfactory results. This convenient and sensitive sensor could be readily extended toward monitoring other small toxic or harmful molecules in food and environment samples.

Keywords Electrochemical sensor · Electrochemical oxidation · Bisphenol A · Carbon nanohorn · Cetyltrimethylammonium bromide

Introduction

Bisphenol A (2,2-bis(4-hydroxyphenyl) propane, BPA), is the key monomer in the synthesis of polycarbonate and epoxy resin products [1, 2]. These materials are extensively used in production of food containers or packaging, inner coating of food cans, beverage cans, water bottles, baby bottles, dental sealants, and drug delivery systems. Owing to the generous use of BPA-based products in daily living, BPA is present in a wide array of food, environment and the bodies of living organisms and humans. Unfortunately, BPA, as one of potent endocrine-disrupting compounds, can interfere with hormonal activities in the growth, thereby giving rise to the sexual dysfunction or differentiation, the impaired immune function, and the enhanced risk of various cancers (e.g., testicular, prostate, and breast cancer) even at very low concentration [3, 4]. U.S. Food and Drug Administration (FDA) estimated that BPA exposure from food contact materials is approximately 2.42 and 0.185 μg/kg bw/day for adults and infants, respectively. The European Food Safety Authority (EFSA) indicated that the current Tolerable Daily Intake (TDI) level for BPA was 4 μg/kg bw/day in January 2015 [5, 6], and the use of BPA in baby bottles was forbidden in all EU-countries, Canada and many other countries due to increasing public concerns over the impact of BPA exposure on infants and children. Therefore, development of convenient, selective, and sensitive analytic

✉ Jing Zhang
jzhang@cczu.edu.cn

✉ Zhidong Chen
zdchen@cczu.edu.cn

[1] School of Petrochemical Engineering, School of Food Science and Technology, Changzhou University, Changzhou 213164, Jiangsu, People's Republic of China

[2] Jiangsu Collaborative Innovation Center of Photovoltaic Science and Engineering, Changzhou University, Changzhou 213164, Jiangsu, People's Republic of China

Published online: 12 February 2018

methods for the detection of BPA is of significant importance for guaranteeing the safety of consumers.

The traditional techniques for the detection of BPA mainly include fluorimetry [7], liquid chromatography [8], gas chromatography [9], capillary electrophoresis [10], and enzyme-linked immunosorbent assay [11]. Despite the fact that the above techniques have a good analytical performance for BPA detection, several disadvantages including relatively expensive instrumentation, advanced technical expertise requirements, time-consuming and complicated procedures have limited their application. Electrochemical techniques have attracted considerable attention for the intrinsic advantages, such as rapid response, high sensitivity, instrument simplicity, and feasibility of miniaturization. Electrochemical sensing for BPA was commonly based on the oxidation signal of BPA on the electrodes [12–21]. Thus, the fabrication of the electrode is a crucial step in the detection of BPA. Various electrodes such as polymers [12], ionic liquids [13], layered double hydroxide [14, 15], nanomaterials [16, 17], and nanomaterial-based composites [18–21] modified electrodes had been exploited to the detection of BPA. However, the preparation of some modified electrodes was relatively complicated, and some modified electrodes suffering from low capacity and conductivity had inefficient performance for the detection of BPA. Alternately, it is of great significance to search an efficient modified electrode possessing high capacity and conductivity for BPA detection.

Chemically modified electrode, as a core component of electrochemical sensors, plays a vital role in electrochemical detection of different compounds [22]. Recently, nano-carbon materials have been proven to be the most attractive nanomaterial in the field of electrochemistry due to the unique mechanical and electronic properties [23]. Carbon nanotube [19], carbon microsphere [24], and graphene [25–28] had been extensively applied to chemically modify onto bare electrodes for improvement and enhancement the performance of electrochemical sensors. CNH is a nano-carbon material with dahlia-flower-like spherical superstructure. CNH has aroused considerable attention in extensive electrocatalytic applications owing to the large surface area, excellent conductivity, plentiful inner nanospaces, and highly defective horns [29–31]. Compared with other carbon materials, CNH is assembled by thousands of graphitic tubules with closed ends with cone-shaped horns, and the oxidation treatment of CNH can produce extensive oxygen-functionalized sites exposed on the cone-shaped tips acting as nanocarriers for loading TiO_2 nanoparticles [32], gold nanoparticles [33], and biomacromolecules [34, 35]. In this work, we have loaded a cationic surfactant monolayer on carboxylic CNH to prepare a functionalized nanocomposite modified electrode for construction electrochemical BPA sensor.

Surfactants, a special class of amphiphilic molecules, have polar heads at one end and long hydrophobic tails at the other. Surfactants have been widely applied in electroanalytical chemistry to improve the properties of the electrode/solution interface [36]. Modification of the electrode surface by a surfactant increased the electron transfer rate between the electrode surface and the analyte and improved the detection limits of electrochemical sensors [37]. Zhou et al. prepared sodium dodecyl benzene sulfonate (SDBS) functionalized graphene for confined electrochemical growth of metal/oxide nanocomposites for fructose sensing, and the designed sensor showed a low detection limit and high sensitivity because of the highly negative charged site and facile charge transfer ability of SDBS [38]. Due to the preconcentration of BPA of didodecyldimethylammonium bromide (DDAB) via hydrophobic interaction, Zhang et al. fabricated an electrochemical and sensitive sensing of BPA based on DDAB modified expanded graphite paste electrodes [39]. Zhang et al. prepared SDBS modified expanded graphite paste electrodes for sensitive and selective determination of dopamine in the presence of ascorbic acid and uric acid because of the electrostatic repulsions between negatively charged ascorbic acid and uric acid and SDBS [40]. Cetyltrimethylammonium bromide (CTAB) is a cationic surfactant in the group of quaternary ammonium compounds. Zhou et al. prepared CTAB-carboxylic walled carbon nanotubes composite for a facile and sensitive electrochemical flavonoids sensor, and the proposed sensor showed enhanced sensitivity due to the long alkane chain in CTAB to adsorb flavonoids [23]. This work describes CTAB functionalized carboxylic carbon nanohorn (CNH) for fabrication a highly sensitive electrochemical BPA sensor.

The CTAB-CNH was conveniently prepared by the adsorption of CTAB monolayer on the surface of CNH via the electrostatic interaction with the assistance of ultrasonication. The electrochemical behavior of CTAB-CNH modified glassy carbon electrode (CTAB-CNH/GCE) for BPA was investigated by cyclic voltammetry. The combination of the advantages of CTAB and CNH made the proposed electrode to show enhanced electrocatalytic activity toward the oxidation of BPA. Based on the high electrocatalytic responses to BPA at CTAB-CNH/GCE, a novel electrochemical sensor was developed for the detection of BPA. The designed sensor showed good performance with a wide linear range, a low detection limit, and had excellent reproducibility, stability, reusability, and selectivity for the detection of BPA. The proposed sensor was successfully applied in the detection of BPA in real plastic product and environmental samples.

Experimental

Materials

Carbon nanohorn (CNH, > 97% purity) was purchased from Nanjing XFNANO Materials Tech Co., Ltd. (China). BPA (99% purity) were obtained from Shanghai Runjie Chemical

Reagent Co., Ltd. (China). Cetyltrimethylammonium bromide (CTAB), chitosan, Na_2HPO_4, and NaH_2PO_4 were purchased from Sinopharm Chemical Reagent Co., Ltd. (China). All the solutions were prepared with twice distilled water. The buffer for assay was 0.1 mol/L phosphate buffer saline (PBS) prepared by mixing stock-standard solution of Na_2HPO_4 and NaH_2PO_4. 0.1 mol/L BPA stock solution was prepared in ethanol and kept in darkness at 277 K.

Apparatus

Transmission electron microscopic (TEM) images of CNH were gained on a JEM-2100 transmission electron microscope (JEOL, Japan). Scanning electron microscopy (SEM) images were obtained on a SUPRA55 scanning electron microscope (Germany). High performance liquid chromatography (HPLC) determinations of BPA in real plastic product samples were carried out on a HPLC system containing a pump (1260 Infinity II isocratic, USA) and a UV-vis detector (1260 Infinity II programmable, USA). Separations were carried out on a Poroshell 120 EC-C_{18} column (15 cm × 4.6 mm, with 2.7 μm particle size) from Agilent (USA) at 298 K. The mobile phase of water and acetonitrile (55:44, *v*/*v*) was delivered at flow rate of 1 mL min^{-1}, the injection volume was 20 μL for all the test solutions, and the detection wavelength was 224 nm [41]. A pHS-3C digital pH meter obtained from Shanghai INESA scientific instrument Co., Ltd. (Shanghai, China) with a combined glass electrode was used to adjust the pH value of the PBS buffer solution, which was used as the supporting electrolyte in the voltammetric experiments. Electrochemical impedance spectroscopy (EIS) was carried out with a VersaSTAT3 electrochemical workstation (Princeton Applied Research, USA) using the three-electrode setup in 0.1 mol/L KCl containing 1 mmol/L $K_3[Fe(CN)_6]/K_4[Fe(CN)_6]$, and the impedance spectra were recorded within the frequency range of 10^{-2}–10^5 Hz. Electrochemical experiments including cycling voltammetry (CV) and differential pulse voltammetry (DPV) were performed with CHI 660E electrochemical workstation (CH Instruments Inc., USA) with a conventional three-electrode cell. A CTAB-CNH/GCE was used as working electrode, a saturated calomel electrode (SCE) and a platinum wire were used as reference electrode and auxiliary electrode, respectively. All the electrochemical measurements were carried out at 298 K.

Preparation of carboxylic CNH

Forty milligrams CNH was dispersed in 60 mL 30% HNO_3 solution, and the resultant mixture was refluxed for 24 h at 140 °C. The resulting suspension was centrifuged and the precipitate was washed thoroughly with water to get carboxylic CNH. Subsequently, 2.0 mg of carboxylic CNH were dispersed in 1.0 mL water to obtain a homogeneous dispersion and the black homogeneous solution was stable at least 3 months.

Preparation of CTAB-CNH and CTAB-CNH suspension

CTAB-CNH was prepared according to the following procedure. Fifteen milligrams CTAB was dispersed in 1 mL carboxylic CNH solution (2 mg/mL). After sonicating for 1 h at 298 K, the suspension solution was centrifuged at 10000 rpm. The precipitate was collected, washed copiously with water for several times to obtain CTAB-CNH.

The resulting CTAB-CNH was redispersed into 1 mL 0.1% chitosan solution containing 1% acetic acid, and followed by sonicating for 10 min at 298 K to get homogeneous CTAB-CNH suspension. As control, CNH suspension was prepared with the same procedure by dispersing carboxylic CNH into chitosan acetic acid solution.

Preparation of CTAB-CNH-modified electrode

The glassy carbon electrode (GCE, 3 mm diameter) was polished successively with 0.3- and 0.05-μm alumina slurry (Beuhler) followed by rinsing thoroughly with doubly distilled water. After successive sonication in 1:1 nitric acid, acetone and distilled water, the electrode was rinsed with distilled water and allowed to dry at room temperature. CTAB-CNH modified GCE (CTAB-CNH/GCE) was prepared by dropping 1 μL of CTAB-CNH suspension on the pretreated GCE, and dried at room temperature. As control, CNH suspension modified GCE (CNH/GCE) was prepared with the same procedure by dropping CNH suspension on the GCE.

Analytical procedure

The analytical procedure mainly contains two steps: accumulation step and stripping step. BPA was firstly accumulated on CTAB-CNH/GCE at the constant potential of 0.3 V for 180 s in 20 mL 0.1 mol/L pH 8.0 PBS buffer solution with different concentration of BPA under stirring. After equilibrating for 30 s, differential pulse voltammograms measurements were obtained from 0.3 to 0.75 V with the pulse amplitude of 50 mV, pulse width of 50 ms, and sampling width of 16.7 ms. Unless otherwise stated, 0.1 mol/L pH 8.0 PBS buffer solution was used as a supporting medium for BPA detection. The data for condition optimization and calibration curve were the average of three measurements.

Sample preparation

Eight real plastic product samples (four types of polycarbonate (PC) drinking package and four types of polyethylene terephthalate (PET) drinking bottle) were purchased from a

local supermarket. The method of sample preparation for extraction of BPA was according to the previously reported method [42]. These samples were precleaned in an ultrasonic bath with acetone, rinsed successively with alcohol, twice distilled water, and then dried. After being cut into small pieces, 2.0 g plastic product pieces and 50 mL twice distilled water were added into a flask fitted with a condenser. The flask was placed in an oil bath at 343 K for 48 h. After cooling to room temperature, the condenser was washed with distilled water. After filtration, the filtrate was collected in a 100-mL volumetric flask and diluted with distilled water. Five microliters sample solution was transferred to the cell containing 0.1 mol/L pH 8.0 PBS buffer solution and analyzed by DPV and HPLC analysis.

Results and discussion

Morphological characterization of CNH, CTAB-CNH, and CTAB-CNH/GCE

Figure 1 shows the TEM images of CNH. Spherical CNH aggregates are densely packed on the surface (Fig. 1a). The amplified TEM image of CNH shows the typical morphology of dahlia-like CNH bundles about 80–100 nm in bundle diameter (Fig. 1b). The cone-shaped tips of CNH could provide good capacity for the adsorption of CTAB and BPA, which could enhance sensitivity for the proposed BPA sensor. After modification with CTAB onto CNH, the mushy configuration of CTAB-CNH reveals that CTAB was attached to CNH (Fig. 1c). The typical SEM images of CTAB-CNH modified GCE showed spherical CTAB-CNH aggregates were well dispersed on the surface of electrode without agglomeration (Fig. 1d), which provided a larger effective contact area for determined compounds.

Electrochemical characterization of bare GCE, CNH/GCE, and CTAB-CNH/GCE

Using $Fe(CN)_6^{3-/4-}$ as a redox probe, the electrochemical behavior of bare GCE and CNH/GCE was separately investigated by CV method (Fig. 2a). A redox peak shapes were obtained at the bare GCE and the peak currents were 33 μA (curve a). The currents of ferricyanide anodic and cathodic peaks at CNH/GCE largely increased to 50 μA (curve b), indicating improved electron transfer and mass transfer, which could be contributed to the high surface area (1263 $m^2\ g^{-1}$) provided by the three dimensional structure of CNH. The result manifests that carbon nanohorn is quite favorable electrode material for the construction of BPA sensor. With the modification of CTAB, the redox current peaks at CTAB-CNH/GCE decreased to 44 μA (curve c). The decrease was ascribed to the blocking the mass transport of CTAB, which further confirmed the successful modification of CNH with CTAB.

Using a $Fe(CN)_6^{3-/4-}$ redox couple as the electrochemical probe, the Nyquist plots of two electrodes in the frequency range from 10^{-2} to 10^5 Hz is shown in Fig. 2b. To analyze the electrode's impedance characteristics a modified Randles equivalent circuit (Fig. 2b inset) was chosen to fit the measured results. The two components of the scheme, Rs and Zw, represent the bulk properties of electrolyte solution and diffusion of the applied redox probe, respectively. The Cdl depends

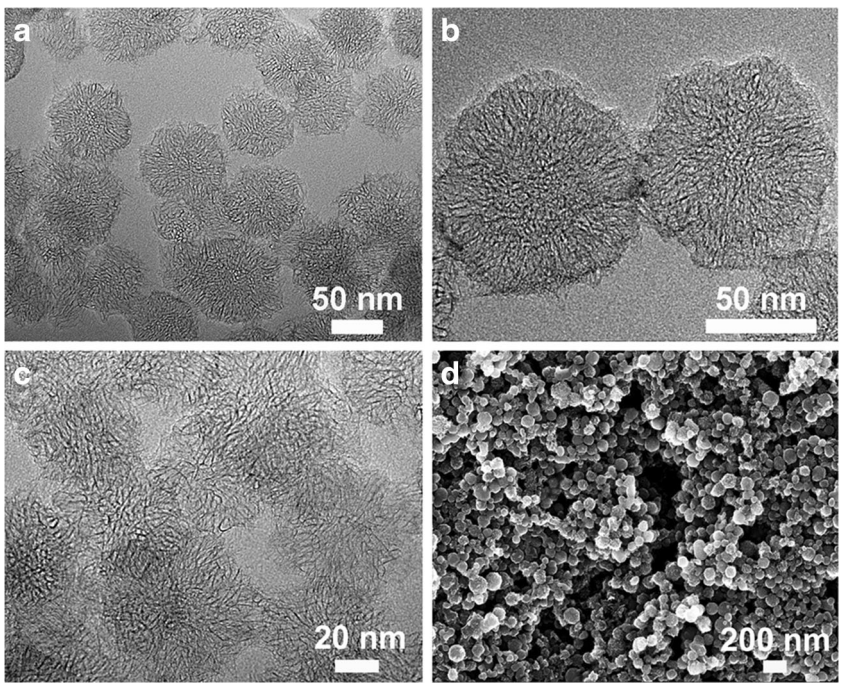

Fig. 1 TEM images of CNH (**a**, **b**) and CTAB-CNH (**c**), and SEM image of CTAB-CNH/GCE (**d**)

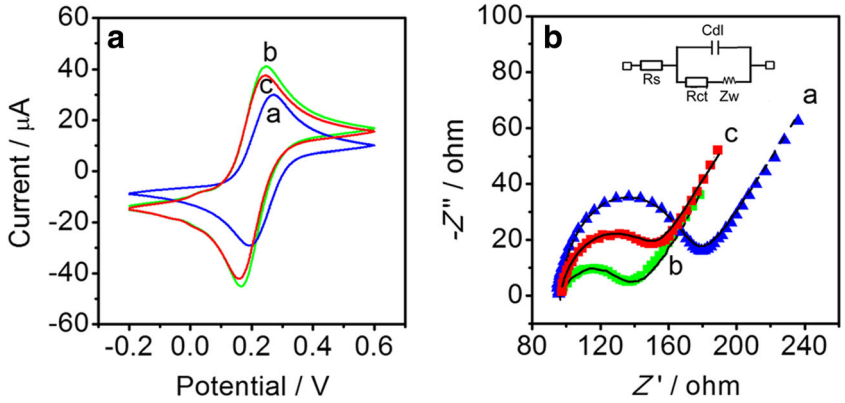

Fig. 2 Cyclic voltammograms (**a**) and EIS recordings (**b**) in 0.1 mol/L KCl containing 1 mmol/L $K_3[Fe(CN)_6]/K_4[Fe(CN)_6]$ at bare GCE (a), CNH/GCE (b), and CTAB-CNH/GCE (c). Scan rate: 50 mV/s

on the dielectric at the electrode/electrolyte interface. At bare GCE the redox process of the probe showed an electron transfer resistance (R_{ct}) of about 75 Ω (curve a). After CNH was coated on the electrode, the resistance decreased to about 40 Ω (curve b), implying that CNH is an excellent electric conducting material. While CTAB-CNH was modified on the GCE, the resistance climbed to approximately 55 Ω (curve c), indicating the effective modification of CNH with CTAB. The result is consistent with the CV test.

Electrochemical responses of BPA at GCE, CNH/GCE, and CTAB-CNH/GCE

Figure 3 shows the electrochemical behaviors of different electrodes after accumulation of 5.0 μmol/L BPA in 0.1 mol/L PBS buffer solution. The CV at GCE showed a stable and well-defined oxidation peak at 0.52 V (curve a), and the peak current was 0.5 μA, which corresponded to the oxidation of hydroxy group of BPA accumulated on GCE into the corresponding quinone. The peak current of CNH/GCE (curve b) was 2.6 times higher response than that of GCE, which can be contributed to the excellent conductivity and capacity of

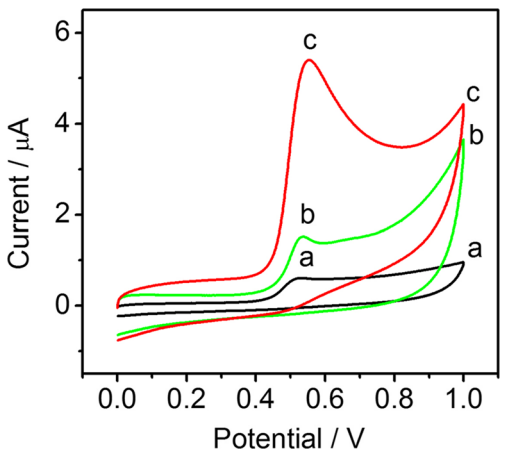

Fig. 3 Cyclic voltammograms at GCE (a), CNH/GCE (b), and CTAB-CNH/GCE (c) in 0.1 mol/L pH 8.0 PBS containing 5.0 μmol/L BPA. Scan rate: 100 mV/s

CNH. Owing to the preconcentration of BPA of the long alkane chain in CTAB via hydrophobic interaction, the peak current of CTAB-CNH/GCE (curve c) exhibited 3.7 times higher response than those of CNH/GCE. The good electrochemical behavior of CTAB-CNH/GCE toward BPA could benefit from the combined enhancement effect of CNH and CTAB.

Optimization of the condition for the CTAB-CNH/GCE fabrication

The concentration of CNH in the preparation of CTAB-CNH/GCE played an important role on BPA detection at CTAB-CNH/GCE. As seen in Fig. 4a, the peak current of 5.0 μmol/L BPA at the resulting CTAB-CNH/GCE increased with the increasing amount of CNH from 1.0 to 2.0 mg/mL, afterwards the peak current decreased as the amount further increased in the range of 2.0–2.5 mg/mL. Therefore, the amount of 2.0 mg/mL for CNH was selected for the preparation of CTAB-CNH.

The analytical performance of the proposed CTAB-CNH/GCE was dependent on the concentration of CTAB used for the preparation of CTAB-CNH. As shown in Fig. 4b, the peak current increased with the increasing amount of CTAB from 5 to 15 mg/mL, afterwards the peak current decreased. The decrease may be due to the lower electrical conductivity of the electrode caused by the higher amount of CTAB. Therefore, the amount of 15 mg/mL for CTAB was selected for the preparation of CTAB-CNH, and further used for CTAB-CNH/GCE fabrication.

In order to improve the stability of CTAB-CNH on GCE, CTAB-CNH was dispersed into chitosan/acetic acid solution, and the suspension was sonicated and dropped on GCE to obtain CTAB-CNH/GCE. The dependence of the amount of chitosan on the oxidation current of BPA at the resulting CTAB-CNH/GCE is shown in Fig. 4c. The peak current increased with the increasing amount of chitosan from 0.5 to 1 mg/mL, afterwards the peak current decreased as the amount further increased. Therefore, the amount of 1 mg/mL for chitosan was selected for the preparation of chitosan acetic acid solution, and further used for CTAB-CNH/GCE fabrication.

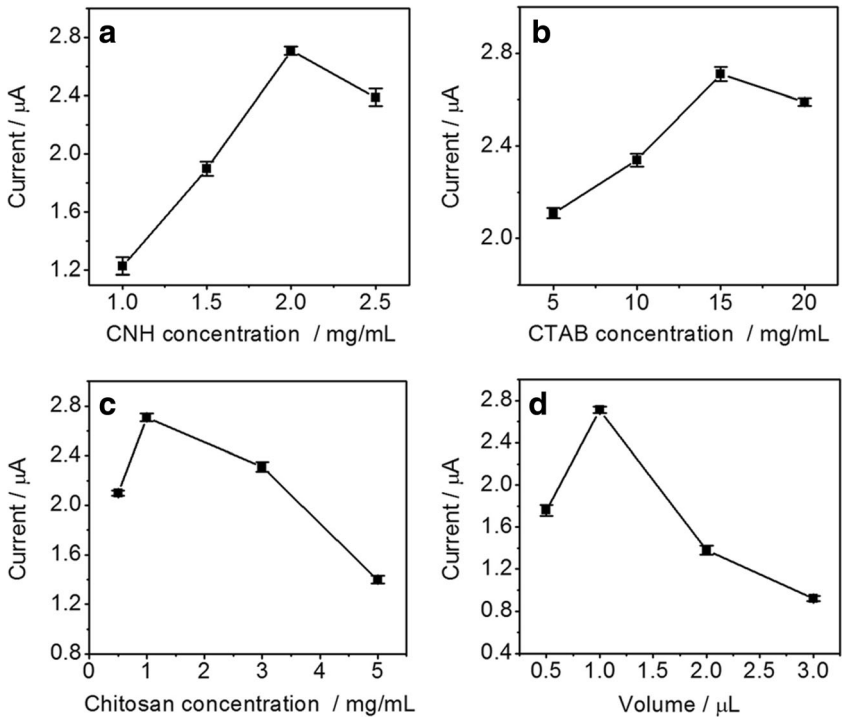

Fig. 4 Influences of the concentrations of CNH (**a**), CTAB (**b**), and chitosan (**c**), and the volume of modification liquid of CTAB-CNH suspension (**d**) on the DPV oxidation peak current of 5.0 μmol/L BPA at CTAB-CNH/GCE. When one parameter changed other parameters were at their optimal values

The volume of modification liquid of CTAB-CNH suspension had a significant influence on the oxidation current of BPA. As shown in Fig. 4d, the peak current increased with the increasing volume of CTAB-CNH suspension from 0.5 to 1 μL, afterwards the peak current decreased in the volume of 1–3 μL. The increase of peak current was due to the fact that more CTAB-CNH on electrode could provide more electroactive sites for BPA electro-oxidation. By contrast, the peak current would likely decrease with the amount of the CTAB-CNH exceeding the critical value owing to the blocking the mass transport of BPA caused by the higher amount of CTAB-CNH. Therefore, the volume of 1.0 μL for CTAB-CNH suspension was selected for the preparation of CTAB-CNH/GCE.

Optimization of accumulation time and accumulation potential

The accumulation efficiency of CTAB-CNH/GCE to 5.0 μmol/L BPA was related to accumulation time and accumulation potential in the accumulation process. As shown in Fig. 5a, the peak current increased continuously as the accumulation time was increasing from 30 to 180 s, and trended to the plateau value at 180 s. With the increasing accumulation potential, the peak current increased and then decreased after 0.3 V (Fig. 5b). Therefore, 180 s and 0.3 V were used as the accumulation time and accumulation potential in the accumulation process, respectively.

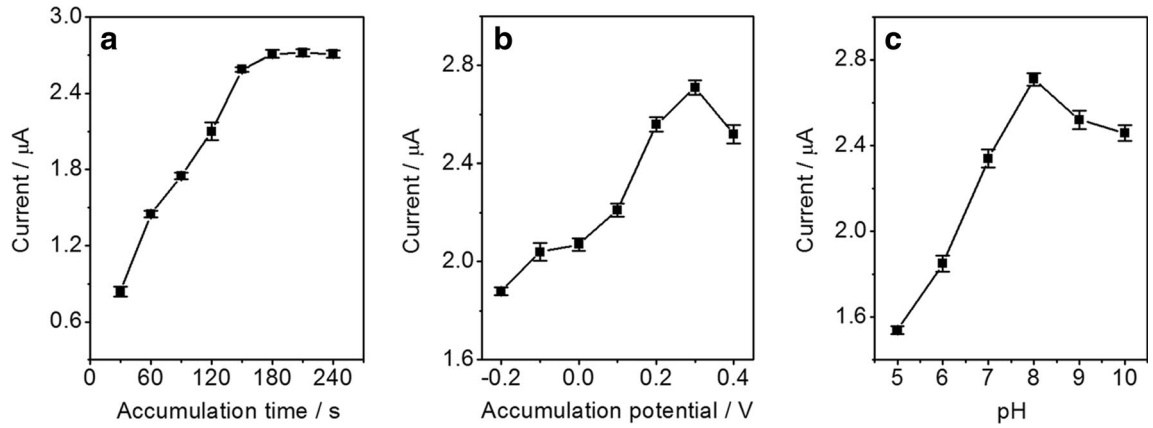

Fig. 5 Effects of accumulation time (**a**), accumulation potential (**b**), and pH value of PBS buffer solution (**c**) on the DPV oxidation peak current of 5.0 μmol/L BPA at CTAB-CNH/GCE. When one parameter changed other parameters were at their optimal values

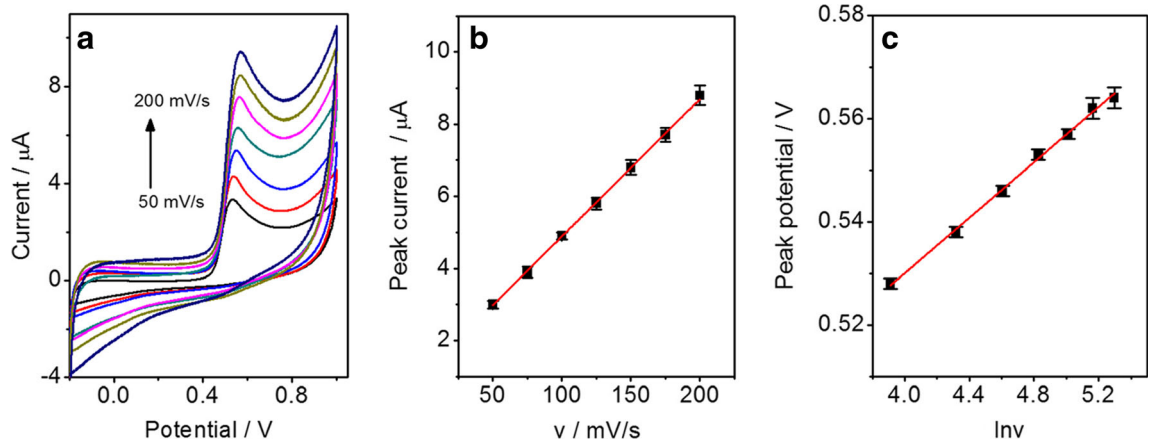

Fig. 6 Cyclic voltammograms (**a**) of 5.0 μmol/L BPA at CTAB-CNH/GCE with different scan rates ranging from 50 to 200 mV/s in 0.1 mol/L PBS buffer solution, and the relationships of peak current and scan rate (**b**) and peak potential and Napierian logarithm of scan rate (ln v)

The effect of pH

The effect of pH value of 0.1 mol/L PBS for the electrochemical detection of 5.0 μmol/L BPA at CTAB-CNH/GCE was investigated over the pH of 5.0–10.0. As seen in Fig. 5c, with an increasing pH from 5.0 to 8.0 the DPV peak current increased, following with a decrease in the pH range of 8.0–10.0. The maximum response pH was lower than the pKa of BPA (pKa = 9.73), which indicated that the nondissociated BPA could be adsorbed better than the dissociated BPA on CTAB-CNH/GCE surface via hydrophobic interaction [23, 43]. Therefore, pH 8.0 of 0.1 mol/L PBS buffer solution was used the supporting electrolyte for the electrochemical detection of BPA.

Effect of scan rate

To further understand the characteristics of CTAB-CNH/GCE, electrochemical behavior of BPA at CTAB-CNH/GCE with different scan rates was investigated. Figure 6a shows the cyclic voltammograms of 5.0 μmol/L BPA at CTAB-CNH/GCE with different scan rates, and the oxidation peak current increased gradually with the increase of scan rate. As seen in Fig. 6b, the peak current increased linearly with the scan rate in the range of 50 to 200 mV/s, and the equation can be expressed as Ipa (μA) = 0.038 v (mV/s) + 1.082 (R^2 = 0.9995). The result indicates that the oxidation of BPA at CTAB-CNH/GCE surface is a typical adsorption-controlled process.

Moreover, the oxidation potential (Epa) was found to shift toward positive value with the scan rate increasing, and a linear relationship between Epa and Napierian logarithm of v (ln v) was also observed (Fig. 6c). The equation was expressed as Epa (V) = 0.0268 ln v (mV/s) + 0.423 (R^2 = 0.9976). For a totally irreversible electrode process, the relationship between Epa and lnv can be expressed by Laviron equation [44]:

$$\mathrm{Epa} = E^0 + \left(\frac{RT}{\alpha nF}\right) In\left(\frac{RTk_s}{\alpha nF}\right) + \left(\frac{RT}{\alpha nF}\right) Inv$$

where α is the electron transfer coefficient, k_s is the standard heterogeneous rate constant, n is the number of transferred electrons, v is scan rate, and E^0 is formal potential, R, T, and F have their usual meanings. Thus, the value of αn can be

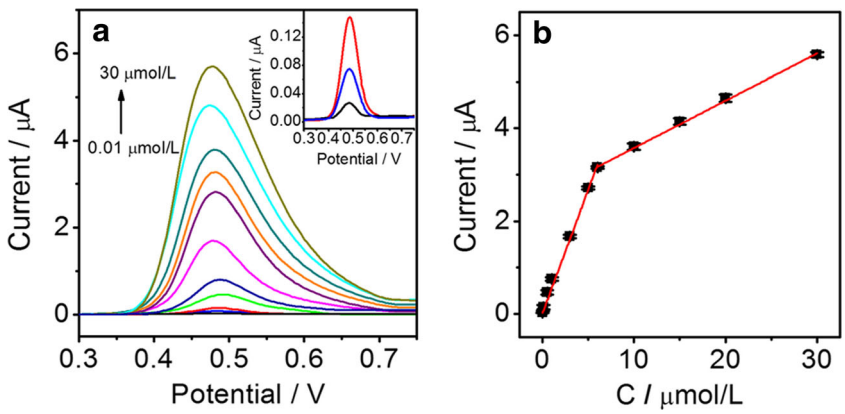

Fig. 7 DPVs of different concentrations of BPA at CTAB-CNH/GCE in 0.1 mol/L pH 8.0 PBS buffer solution (**a**), inset: amplified response curve, and calibration curve for BPA sensing at CTAB-CNH/GCE (**b**)

Table 1 The comparison of detection performance of CTAB-CNH/GCE-based sensor with other sensors

Electrode	Linear range (μmol/L)	Limit of detection (nmol/L)	Refs.
PEDOT/BMIMBr/SPCE	0.1–500	20	[12]
NiO/CNT/IL/CPE	0.08–500	40	[13]
ELDH/GCE	0.02–1.51	6.8	[14]
NPG/GCE	0.1–50	12.1	[16]
Na-doped WO_3 nanorods/CPE	0.08–22.5	28	[17]
AuPd nanoparticle /GN/GCE	0.05–10	8	[18]
CNT/$Li_4Ti_5O_{12}$/ GCE	0.1–10	78	[19]
Cu_2O-rGO/GCE^h	0.1–80	53	[20]
CNT modified AuNP-paper	0.88–88	131	[21]
CTAB-CNH/GCE	0.01–30	5.6	This work

PEDOT Poly(3,4-ethylenedioxythiophene), *BMIMBr* 1-butyl-3-methylimidazolium bromide, *SPCE* screen printed carbon electrode, *CNT* carbon nanotube, *IL* ionic liquid, *CPE* carbon paste electrode, *ELDH* Exfoliated Ni_2Al layered double hydroxide nanosheet, *GCE* glassy carbon electrode, *NPG* nanoporous Gold, *GN* graphene nanosheet, *rGO* reduced graphene oxide, *AuNP* gold nanoparticle, *CTAB-CNH* cetyltrimethylammonium bromide functional carbon nanohorn

calculated from the slope of Epa vs lnv. Therefore, the value of αn was 0.958. (taking $R = 8.314$ J/Kmol, $T = 298$ K, $F = 96{,}485$ C/mol). Generally, α was assumed to be 0.5 for a totally irreversible electrode process. So the number of transferred electrons in the electro-oxidation of BPA at CTAB-CNH/GCE surface was 1.91. This result shows the electro-oxidation process of BPA is a two-electron and two-proton process, which is in agreement with other published reports [14, 17, 39, 43]. The electro-oxidation process could be described as follows:

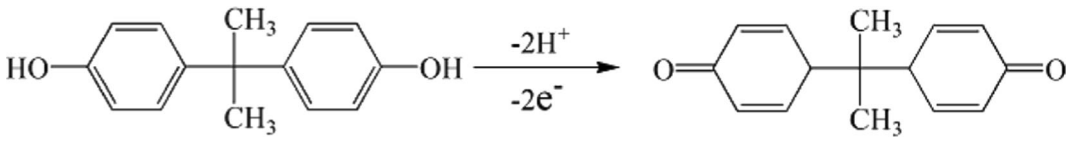

Linear range and detection limit

In order to evaluate the analytical performance of the prepared electrochemical sensor, different concentrations of BPA standard solution were measured by DPV method. Figure 7 displays the DPVs of different concentrations of BPA at CTAB-CNH/GCE in 0.1 mol/L PBS. The peak current of BPA at CTAB-CNH/GCE increased with the increasing concentration of BPA (Fig. 7a). As shown in Fig. 7b, the linear concentration range of BPA at CTAB-CNH/GCE was from 0.01 to 30 μmol/L, and the regression equations could be expressed as Ipa (μA) = 0.532 C (μmol/L) + 0.018 ($R^2 = 0.9965$) and Ipa (μA) = 0.102 C (μmol/L) + 2.554 ($R^2 = 0.9985$) in the range of 0.01–6.0

Scheme 1 The schematic preparation and mechanism of CTAB-CNH/GCE-based electrochemical BPA sensor

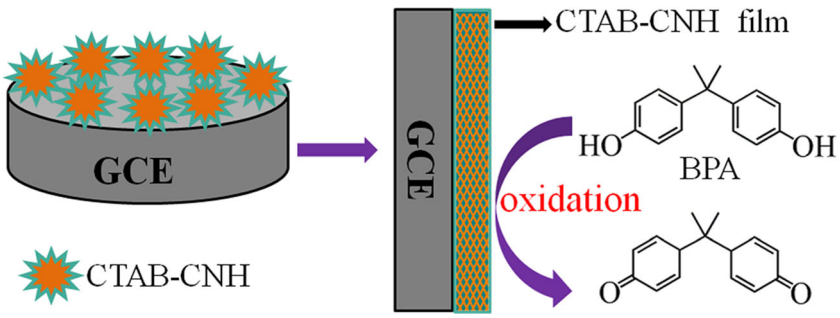

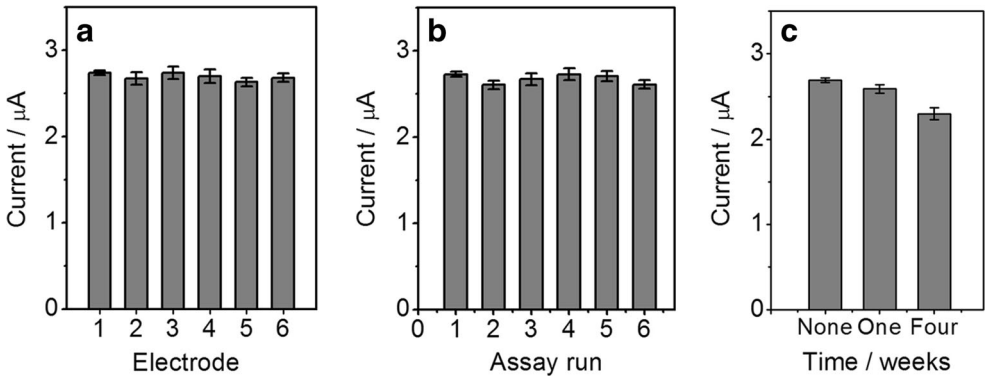

Fig. 8 DPV peak currents of 5.0 μmol/L BPA at CTAB-CNH/GCE in reproducibility (**a**), reusability (**b**), and stability (**c**) experiments

and 6.0–30 μmol/L, respectively. At low BPA levels, the local concentration at the proposed electrode surface is rapidly depleted as the substrate is converted into product by the catalytic action of the proposed electrode, resulting in a high sensitivity of the electrode response. At higher BPA concentrations, it takes a long time to transfer substrate to the proposed electrode, and the reaction proceeds over a larger time window. Moreover, the possibility of fouling of the electrode surface by the reaction products the reaction product may be fouled on the surface of the proposed electrode. These results lead to a lower slope at higher BPA concentrations. The detection limit for BPA was calculated as 5.6 nmol/L at a ratio of signal to noise of 3. The detection performance of the sensor fabricated in this work was compared with other sensors. As shown in Table 1, it is clear that CTAB-CNH/GCE-based sensor had a wider linear range and a lower detection limit. The good performance of CTAB-CNH/GCE-based sensor for BPA benefits from the combined enhancement effect of preconcentration of BPA in the long alkane chain of CTAB via hydrophobic interaction and excellent capacity and electrocatalytic activity of CNH (Scheme 1).

Table 2 Interference effects on the detection of 5.0 μmol/L BPA in pH 7.0 PBS

Interference	Concentration (μmol L^{-1})	Signal change (%)	RSD (%)
Zn^{2+}	500	−2.4	2.5
K^{+}	500	+0.4	3.5
Cu^{2+}	500	−2.0	3.4
Fe^{3+}	500	−1.1	3.8
Cl^{-}	500	−2.5	3.0
NO_3^{-}	500	−1.6	2.9
SO_4^{2-}	500	−1.3	2.6
Phenol	250	−1.6	1.1
Hydroquinone	250	−0.7	1.4
o-Nitrophenol	250	+3.1	2.9
p-Nitrophenol	250	+1.1	3.1
Bisphenol B	5	+3.7	4.9
Bisphenol F	5	+4.6	1.7

Reproducibility, reusability, and stability

The reproducibility, reusability, and stability of CTAB-CNH/GCE were investigated under the optimized conditions. The reproducibility of CTAB-CNH/GCE was examined in the solution containing of 5.0 μmol/L BPA, and the relative standard deviation (RSD) of current signals at six independently prepared CTAB-CNH/GCE was 1.54% (Fig. 8a), indicating an excellent repeatability. The regeneration of CTAB-CNH/GCE was carried out by cycling voltammetry from − 0.2 to 1.0 V in 0.1 mol/L pH 8.0 PBS for ten times. The as-renewed CTAB-CNH/GCE could restore 95.2% of the initial value for BPA after five assay runs, which proved good reusability of electrode (Fig. 8b). When CTAB-CNH/GCE was not in use, it was stored at 278 K. Ninety-six percent and 85% of the initial responses of CTAB-CNH/GCE for BPA were remained after one and 3 weeks when using once per 7 days (Fig. 8c), respectively, indicating an acceptable stability of CTAB-CNH/GCE.

Interference studies

The specificity of the designed sensor was evaluated by challenging it against other usual phenolics and inorganic salt ions and two other bisphenols. The results demonstrated 5.0 μmol L^{-1} BPA were not affected by 50-fold concentration of phenol, hydroquinone, *o*-nitrophenol, *p*-nitrophenol, 100-fold concentration of K^{+}, Cu^{2+}, Fe^{3+}, Zn^{2+}, Cl^{-}, SO_4^{2-}, and NO_3^{-}, and same concentration of bisphenol B and bisphenol F, and the responses of CTAB-CNH/GCE to BPA changed less than 5.0% (Table 2). CNH provided a mechanically stable, conducting and large effective contact platform for the adsorption of CTAB, and the hybrid component increased selectivity of CTAB-CNH composite modified electrode based sensor toward BPA.

Table 3 Detection of BPA in real plastic product samples

Sample	Measured by proposed method					Measured by HPLC				
	Original	Added (μM)	Found (μM)	RSD (%)	Recovery (%)	Original	Added (μM)	Found (μM)	RSD (%)	Recovery(%)
PC drinking package 1	None	0.100	0.0980	2.53	98.0	None	0.100	0.106	4.17	106
PC drinking package 2	None	0.100	0.0965	2.86	96.5	None	0.100	0.101	3.82	101
PC drinking package 3	None	0.100	0.0993	3.83	99.3	None	0.100	0.0962	3.65	96.2
PC drinking package 4	None	0.100	0.103	3.16	103	None	0.100	0.108	3.13	108
PET drinking bottle 1	None	0.100	0.100	3.35	100	None	0.100	0.103	2.76	103
PET drinking bottle 2	None	0.100	0.102	1.65	102	None	0.100	0.0974	4.68	97.4
PET drinking bottle 3	None	0.100	0.0958	4.32	95.8	None	0.100	0.0938	4.68	93.8
PET drinking bottle 4	None	0.100	0.103	3.66	103	None	0.100	0.104	3.34	104

Analysis of food samples

To evaluate the potential application, the designed sensor was employed for in situ detection of trace amount of BPA in eight real plastic samples (four types of PC drinking package and four types of PET drinking bottle). Recovery testing was carried out to demonstrate the validity of the proposed method. The obtained recoveries of the proposed sensor for BPA in two real plastic samples were 95.8 and 103% (Table 3). For comparison, the concentrations of BPA in these samples were also detected by HPLC. In HPLC analysis, the linear concentration range of BPA was from 0.01 to 0.5 μmol/L, and the regression equation could be expressed as A (μV·s) = 4781.9 C (μmol/L) + 688.2 (R^2 = 0.9928). The detection limit for BPA was calculated as 0.006 μmol/L at a ratio of signal to noise of 3. As shown in Table 3, the assay results obtained by both methods showed a good agreement. This result suggests the good accuracy of the proposed sensor. Thus, the present sensor could satisfy the need for detection of BPA in real plastic product samples.

Conclusions

In this work, a sensitive and selective electrochemical BPA sensor was developed using the CTAB functionalized CNH modified electrode. Because of the combination of the advantages of the preconcentration of BPA of the long alkane chain in CTAB via hydrophobic interaction, and high conductivity and capacity of CNH, the CTAB-CNH/GCE showed enhanced electrocatalytic activity toward the oxidation of BPA. Based on the electrocatalytic activity to BPA, a sensor for BPA was constructed based on CTAB-CNH/GCE. The proposed sensor for determination of BPA had a wide linear range, a low detection limit, acceptable fabrication reproducibility and stability, and was successfully applied to detect BPA in real plastic samples. The CTAB-CNH opens an insight for functionalization of CNH, and has a great potential for multiple applications in electronic biological or clinical target devices.

Funding information This work was financially supported by the Natural Science Foundation of Changzhou (CE20165047), State Key Laboratory of Analytical Chemistry for Life science (SKLACLS1403), Advanced Catalysis and Green Manufacturing Collaborative Innovation Center (Changzhou University, 213164), and a Project Funded by the Priority Academic Program Development of Jiangsu Higher Education Institutions.

References

1. Ballesteros-Gómez A, Rubio S, Pérez-Bendito D (2009) Analytical methods for the determination of bisphenol A in food. J Chromatogr A 1216:449–469
2. Staples CA, Dorn PB, Klecka GM, O'Block S T, Harris LR (1998) A review of the environmental fate, effects, and exposures of biophenal A. Chemosphere 36:2149–2173
3. Vandenberg L N, Maffini M V, Sonnenschein C, Rubin B S, Soto A M (2009) Bisphenol-A and the great divide: a review of controversies in the field of endocrine disruption. Endocr Rev 30:75–95
4. Hengstler JG, Foth H, Gebel T, Kramer PJ, Lilienblum W, Schweinfurth H, Volkel W, Wollin KM, Gundert-Remy U (2011) Critical evaluation of key evidence on the human health hazards of exposure to bisphenol A. Crit Rev Toxicol 41:263–291
5. EFSA (European Food Safety Authority) (2015) Scientific opinion on the risks to public health related to the presence of bisphenol A (BPA) in foodstuffs: executive summary. EFSA J 13:(1)3978, 23. https://doi.org/10.2903/j.efsa.2015.3978
6. Alonso-Magdalena P, Ropero AB, Soriano S, Quesada I, Nadal A (2010) Bisphenol-A: a new diabetogenic factor? Horm. Int. J. Endocrinol Metab 9:118–126
7. Liu GL, Chen Z, Jiang XY, Feng DQ, Zhao JY, Fan DH, Wang W (2016) In-situ hydrothermal synthesis of molecularly imprinted polymerscoated carbon dots for fluorescent detection of bisphenol A. Sensors Actuators B Chem 228:302–307
8. Qi LL, Wang YH, Li YJ, Zheng GX, Li CP, Su HZ (2015) Microfluidic aqueous two-phase extraction of bisphenol A using ionic liquid for high-performance liquid chromatography analysis. Anal Bioanal Chem 407(13):3617–3625. https://doi.org/10.1007/s00216-015-8572-y
9. Zhang ZL, Rhind SM, Kerr C, Osprey M, Kyle CE (2011) Selective pressurized liquid extraction of estrogenic compounds in soil and

analysis by gas chromatography–mass spectrometry. Anal Chim Acta 685:29–35
10. Alsudir S, Iqbal Z, Lai EPC (2012) Competitive CE-UV binding tests for selective recognition of bisphenol A by molecularly imprinted polymer particles. Electrophoresis 33:1255–1262
11. Maiolini E, Ferri E, Pitasi AL, Montoya A, Di GM, Errani E, Girotti S (2014) Bisphenol A determination in baby bottles by chemiluminescence enzyme-linked immunosorbent assay, lateral flow immunoassay and liquid chromatography tandem mass spectrometry. Analyst 139(1):318–324. https://doi.org/10.1039/C3AN00552F
12. Wang JY, Su YL, Wu BH, Cheng SH (2016) Reusable electrochemical sensor for bisphenol A based on ionic liquid functionalized conducting polymer platform. Talanta 147:103–110. https://doi.org/10.1016/j.talanta.2015.09.035
13. Nikahd B, Khalilzadeh MA (2016) Liquid phase determination of bisphenol A in food samples using novel nanostructure ionic liquid modified sensor. J Mol Liq 215:253–257. https://doi.org/10.1016/j.molliq.2015.12.003
14. Zhan TR, Song Y, Tan ZW, Hou WG (2017) Electrochemical bisphenol A sensor based on exfoliated Ni_2Al-layereddouble hydroxide nanosheets modified electrode. Sensors Actuators B Chem 238:962–971. https://doi.org/10.1016/j.snb.2016.07.151
15. Baig N, Sajid M (2017) Applications of layered double hydroxides based electrochemical sensors for determination of environmental pollutants: a review. Trends Environ Anal Chem 16:1–5. https://doi.org/10.1016/j.teac.2017.10.003
16. Yan XP, Zhou CQ, Yan Y, Zhou Y (2015) A simple and renewable nanoporous gold-based electrochemical sensor for bisphenol A detection. Electroanalysis 27(12):2718–2724. https://doi.org/10.1002/elan.201500349
17. Zhou YZ, Yang LH, Li SH, Dang Y (2017) A novel electrochemical sensor for highly sensitive detection of bisphenol A based on the hydrothermal synthesized Na-doped WO_3 nanorods. Sensors Actuators B Chem 245:238–246. https://doi.org/10.1016/j.snb.2017.01.034
18. Su BY, Shao HL, Li N, Chen XM, Cai ZX, Chen X (2017) A sensitive bisphenol A voltammetric sensor relying on AuPd nanoparticles/graphene composites modified glassy carbon electrode. Talanta 166:126–132. https://doi.org/10.1016/j.talanta.2017.01.049
19. Wang W, Yang X, Gu YX, Ding CF, Wan J (2015) Preparation and properties of bisphenol A sensor based on multiwalled carbon nanotubes/$Li_4Ti_5O_{12}$-modified electrode. Ionics 21(3):885–893. https://doi.org/10.1007/s11581-014-1217-x
20. Shi RG, Liang J, Zhao ZS, Liu AF, Tian Y (2017) An electrochemical bisphenol A sensor based on one step electrochemical reduction of cuprous oxide wrapped graphene oxide nanoparticles modified electrode. Talanta 169:37–43
21. Li HY, Wang W, Lv Q, Xi GC, Bai H, Zhang Q (2016) Disposable paper-based electrochemical sensor based on stacked gold nanoparticles supported carbon nanotubes for the determination of bisphenol A. Electrochem Commun 68:104–107. https://doi.org/10.1016/j.elecom.2016.05.010
22. Mizuguchi H, Sasaki K, Ichinose H, Seino S, Sakurai J, Iiyama M, Kijima T, Tachibana K, Nishina T, Takayanagi T, Shida J (2017) A triple-electrode based dual-biosensor system utilizing track-etched microporous membrane electrodes for the simultaneous determination of L-lactate and D-glucose. Bull Chem Soc Jpn 90:1211–1216
23. Liang ZX, Zhai HY, Chen ZG, Wang SQ, Wang HH, Wang SM (2017) A sensitive electrochemical sensor for flavonoids based on amulti-walled carbon paste electrode modified by cetyltrimethylammonium bromide-carboxylic multi-walled carbon nanotubes. Sensors Actuators B Chem 244:897–906. https://doi.org/10.1016/j.snb.2016.12.108
24. Zhu GB, Gai PB, Yang Y, Zhang XH, Chen JH (2012) Electrochemical sensor for naphthols based on gold nanoparticles/hollow nitrogen-doped carbon microsphere hybrids functionalized with SH-β-cyclodextrin. Anal Chim Acta 723:33–38
25. Zhang X, Wu L, Zhou JW, Zhang XH, Chen JH (2015) A new ratiometric electrochemical sensor for sensitive detection of bisphenol A based on poly-β-cyclodextrin/electroreduced graphene modified glassy carbon electrode. J Electroanal Chem 742:97–103. https://doi.org/10.1016/j.jelechem.2015.02.006
26. Bollella P, Fusco G, Tortolini C, Sanzò G, Favero G, Gorton L, Antiochia R (2017) Beyond graphene: electrochemical sensors and biosensors for biomarkers detection. Biosens Bioelectron 89:152–166
27. Zhang RZ, Chen W (2017) Recent advances in graphene-based nanomaterials for fabricating electrochemical hydrogen peroxide sensors. Biosens Bioelectron 89(Pt 1):249–268. https://doi.org/10.1016/j.bios.2016.01.080
28. Khan AH, Ghosh S, Pradhan B, Dalui A, Shrestha LK, Acharya S, Ariga K (2017) Two-dimensional (2D) nanomaterials towards electrochemical nanoarchitectonics in energy-related applications. Bull Chem Soc Jpn 90:627–648
29. Nakamura M, Tahara Y, Fukata S, Zhang MF, Yang M, Iijima S, Yudasaka M (2017) Significance of optimization of phospholipid poly(ethylene glycol) quantity for coating carbon nanohorns to achieve low cytotoxicity. Bull Chem Soc Jpn 90:662–666
30. Urita KM, Seki S, Utsumi S, Noguchi D, Kanoh H, Tanaka H, Hattori Y, Ochiai Y, Aoki N, Yudasaka M, Iijima S, Kaneko K (2006) Effects of gas adsorption on the electrical conductivity of single-wall carbon nanohorns. Nano Lett 6(7):1325–1328. https://doi.org/10.1021/nl060120q
31. Bracamonte MV, Melchionna M, Giuliani A, Nasi L, Tavagnacco C, Prato M, Fornasiero P (2016) H_2O_2 sensing enhancement by mutual integration of single walled carbon nanohorns with metal oxide catalysts: the CeO2 case. Sensors Actuators B Chem 239:923–932
32. Tu WW, Lei JP, Ding L, Ju HX (2009) Sandwich nanohybrid of single-walled carbon nanohorns–TiO_2–porphyrin for electrocatalysis and amperometric biosensing towards chloramphenicol. Chem Comm 28:4227–4229. https://doi.org/10.1039/b906876g
33. Zhao CR, Wu J, Ju HX, Yan F (2014) Multiplexed electrochemical immunoassay using streptavidin/nanogold/carbon nanohorn as a signal tag to induce silver deposition. Anal Chim Acta 847:37–43. https://doi.org/10.1016/j.aca.2014.07.035
34. Zhang J, Lei JP, Xu CL, Ding L, Ju HX (2010) Carbon nanohorn sensitized electrochemical immunosensor for rapid detection of microcystin-LR. Anal Chem 82(3):1117–1122. https://doi.org/10.1021/ac902914r
35. Zhang J, Song XH, Xiong ZB, Dong HF, Wang WC, Chen ZD (2017) Nanogold/Bi_2S_3 nanorods catalyzed silver deposition for carbon nanohorns-enhanced electrochemical immunosensing of Escherichia coli O157:H7. J Electrochem Soc 164:H1–H7
36. Deng P, Xu Z, Feng Y (2012) Highly sensitive and simultaneous determination of ascorbic acid and rutin at an acetylene black paste electrode coated with cetyltrimethyl ammonium bromide film. J Electroanal Chem 683:47–54. https://doi.org/10.1016/j.jelechem.2012.08.002
37. Goyal RN, Bishnoi S (2010) Effect of single walled carbon nanotube–cetyltrimethyl ammonium bromide nanocomposite film modified pyrolytic graphite on the determination of betamethasone in human. Colloid Surf. B: Biointerfaces 77(2):200–205. https://doi.org/10.1016/j.colsurfb.2010.01.024
38. Zhou SH, Wei DL, Shi HY, Feng X, Xue KW, Zhang F, Song WB (2013) Sodium dodecyl benzene sulfonate functionalized graphene for confined electrochemical growth of metal/oxide nanocomposites for sensing application. Talanta 107:349–355

39. Zhang J, Ma S, Wang WC, Chen ZD (2016) Electrochemical sensing of bisphenol A by a didodecyldimethylammonium bromide-modified expanded graphite paste electrode. J AOAC Int 99(4): 1066–1072. https://doi.org/10.5740/jaoacint.16-0072
40. Zhang J, Song XH, Ma S, Wang X, Wang WC, Chen ZD (2017) A novel sodium dodecyl benzene sulfonate modified expanded graphite paste electrode for sensitive and selective determination of dopamine in the presence of ascorbic acid and uric acid. J Electroanal Chem 795:10–16. https://doi.org/10.1016/j.jelechem.2017.04.035
41. Rezaee M, Yamini Y, Shariati EA, Shamsipur M (2009) Dispersive liquid–liquid microextraction combined with high-performance liquid chromatography-UV detection as a very simple, rapid and sensitive method for the determination of bisphenol A in water samples. J Chromatogr A 1216:1511–1514
42. Li YG, Gao Y, Cao Y, Li HM (2012) Electrochemical sensor for bisphenol A determination based on MWCNT/melamine complex modified GCE. Sensors Actuators B Chem 171–172:726–733
43. Zhou WS, Sun C, Zhou YB, Yang XD, Yang WB (2014) A facial electrochemical approach to determinate bisphenol A based on graphene-hypercrosslinked resin MN202 composite. Food Chem 158:81–87
44. Laviron E (1974) Adsorption, autoinhibition and autocatalysis in polarography and in linear potential sweep voltammetry. Electroanal Chem Interracial Electrochem 52(3):355–393. https://doi.org/10.1016/S0022-0728(74)80448-1